Radiation Physics and Chemistry 232 (2025) 112665

Contents lists available at ScienceDirect

Radiation Physics and Chemistry

journal homepage: www.elsevier.com/locate/radphyschem

Self-attenuation effect correction methods employed for gamma-ray spectrometry: A critical review study

A. Barba-Lobo [a,b,*]

[a] Radiation Physics and Environment Group (FRYMA), Department of Integrated Sciences, Center for Natural Resources, Health and Environment (RENSMA), University of Huelva, Huelva, 21071, Spain
[b] Department of Medical Radiation Sciences, Institute of Clinical Sciences, Sahlgrenska Academy at University of Gothenburg, Gothenburg, SE-413 45, Sweden
[*] Radiation Physics and Environment Group (FRYMA), Department of Integrated Sciences, Center for Natural Resources, Health and Environment (RENSMA), University of Huelva, Huelva, 21071, Spain

ARTICLE INFO

Handling Editor: Dr. Chris Chantler

Keywords:
Self-attenuation
Gamma-ray spectrometry
Cutshall model
Appleby model
Monte Carlo-based-simulation codes
Full-energy peak efficiency

ABSTRACT

The usage of gamma-ray spectrometry has become generalized due to several important advantages that offers versus other radiometric techniques such as alpha-particle spectrometry or liquid scintillation counting. When using gamma-ray spectrometry, the full-energy peak efficiency, FEPE, must be accurately and precisely obtained for a wide range of sample chemical compositions, apparent densities and thicknesses, as well as geometries and energies. For this, the self-attenuation effect corrections must be properly applied for each case in order to transform the calibration sample FEPE into problem sample FEPE. Nowadays, different experimental and simulated methodologies such as Cutshall and Appleby models, and LabSOCS, EFFTRAN, DETEFF, PENELOPE and Geant4, respectively, are generally applied to obtain the problem sample FEPE. However, in many cases, self-attenuation effect corrections can be not properly applied. For this reason, the aim of this study is to comprehensively critical review many different experimental and simulated methodologies usually used to apply self-attenuation effect corrections, offering exhaustive discussions about their proper use as well as proposals to improve many different aspects related to them, and making deep comparisons among their advantages and disadvantages. Moreover, an exhaustive comparison among FEPEs obtained using experimental and simulated methodologies was addressed. In the case of the sample pretreatment, this study also offers a wide discussion of many aspects related to their homogenization process regarding the chemical composition and compaction. In addition, the proper selection of the multielement technique for the major element concentrations is also widely discussed in this study, where an accurate measurement of major element concentrations is essential to properly obtain the sample mass attenuation coefficient which is needed to apply self-attenuation effect corrections.

1. Introduction

Nowadays the gamma-ray spectrometry has become one of the main radiometric techniques for the measurement of both natural and artificial radionuclides such as ^{238}U (via ^{234}Th), ^{226}Ra (via its emission of 186 keV or its daughters: ^{214}Pb and ^{214}Bi), ^{210}Pb, ^{228}Ra (via ^{228}Ac), ^{228}Th (via ^{212}Pb, ^{212}Bi or ^{208}Tl) and ^{40}K, and ^{241}Am, ^{152}Eu, $^{137,\ 134}$Cs, ^{133}Ba, ^{131}I, ^{65}Zn, $^{60,\ 57}$Co and ^{54}Mn, respectively (Barba-Lobo et al., 2023a; Barba-Lobo et al., 2023b; Moradi et al., 2019). The determination of radionuclides using gamma-ray spectrometry has several advantages versus other radiometric techniques such as alpha-particle spectrometry or liquid scintillation counting (Gačnika et al., 2019), where for gamma-ray spectrometry, non-need for chemical separation or use of acids and reagents, and less time-consuming working in laboratory.

However, when measuring radionuclides using gamma-ray spectrometry, the full-energy peak efficiency (*FEPE*) must be accurately and precisely determined for a wide range of sample matrices using different types of geometries, and sample volumes and thicknesses (Barba-Lobo et al., 2023b; Barba-Lobo et al., 2021b; Barba-Lobo and Bolívar, 2022). In the case of measuring a sample (problem sample) very different to the sample employed for the efficiency calibration (calibration sample) regarding their chemical composition and apparent densities, using the same geometry and sample thickness for both samples, the photons emitted by the sample are going to be differently self-attenuated (Barba-Lobo and Bolívar, 2022). For this reason, the self-attenuation effect correction, f_a, is essential when calculating the *FEPE* for a

E-mail addresses: alejandro.barba@dci.uhu.es, alejandro.barba@dci.uhu.es.

https://doi.org/10.1016/j.radphyschem.2025.112665
Received 6 January 2025; Received in revised form 13 February 2025; Accepted 27 February 2025
Available online 28 February 2025

problem sample matrix very different from the calibration sample matrix, where f_a generally depends on the chemical compositions and apparent densities of the problem and calibration samples, the problem and calibration samples' thickness and radius, where thickness and radius are generally considered the same for both samples, and the angle formed between the emitted photon trajectory and coaxial or radial detector axis for coaxial or well-type detectors, respectively (Barba-Lobo et al., 2021a, 2021b). The f_a dependence can be generally written as follows:

$$f_a = \frac{\varepsilon_p}{\varepsilon_c} = f_a\left(\eta_p, \eta_c, \rho_p, \rho_c, h_c, h_p, r_c, r_p\theta\right) \quad (1)$$

where ε_p and ε_c are the *FEPEs* obtained for problem and calibration samples, respectively, at a specific gamma emission energy, E_γ, η_p and η_c are their mass attenuation coefficients at that specific E_γ, that can be obtained through their respective chemical compositions and the mass attenuation coefficient of each element (Barba-Lobo et al., 2021c), ρ_p and ρ_c are their apparent densities, θ is the angle formed between the emitted photons trajectories and the coaxial or radial detector axis (for coaxial or well-type detectors, respectively), h_c and h_p are the calibration and problem samples thickness , and r_c and r_p are their radius.

This type of *FEPE* correction is more needed when decreasing E_γ since the sample mass attenuation coefficient has an exponential behavior when decreasing E_γ (Barba-Lobo et al., 2021c). However, for high energies, that is, $E_\gamma > 150$ keV, the usage of f_a is sometimes also essential since for problem samples whose chemical compositions and apparent densities are quite different from those related to the calibration sample, the self-attenuation effect is going to be relatively different for problem and calibration samples.

The proper self-attenuation application requires a previous accurate and precise knowledge of the chemical composition and apparent density of both problem and calibration samples. In the case of the of the sample chemical composition, only major elements, that is, concentrations higher than 0.1%, are going to relatively contribute to the sample mass attenuation coefficient, where their contributions do not only depend on their proportions in the samples but also on their mass attenuation coefficients. Therefore, multielement techniques such as X-ray fluorescence (XRF) (De Francesco et al., 2018), Inductively-Coupled Plasma Mass Spectrometry (ICP-MS) including an extension for upper limit of detection (Liao et al., 2019) or Inductively-Coupled Plasma Optical Emission Spectroscopy (ICP-OES) (Karasaka, 2021) can be used for the obtention of major element concentrations in order to determine the sample mass attenuation coefficient. In the case of very crystalline samples, that is, whose amorphous fraction can be neglected, X-ray diffraction (XRD) can be another option to determine concentrations of major elements using Rietveld method.

Regarding the methods applied when correcting self-attenuations effects, they can be generally classified into two groups: 1. experimental methods using analytical functions and 2. simulated methods using programming codes based on Monte Carlo. In the case of experimental methods, Cutshall and Appleby models are usually applied when measuring samples using coaxial and well-type detectors, respectively. However, these models have relatively limited validity ranges for application in the case of problem sample matrices quite different from calibration sample matrices, which is especially true at energies less than 150 keV (Barba-Lobo et al., 2021c). In the case of using simulation codes, for example, LabSOCS, EFFTRAN, DETEFF, PENELOPE or Geant4, they are generally more robust than experimental procedures but a characterization of the gamma detectors is previously needed.

Therefore, the application of self-attenuation effect corrections has become an issue which is sometimes quite complicated to be properly solved. For this reason, this review study aims to analyze in depth the different experimental and simulated methods that are usually employed to correct self-attenuation effects, discussing advantages and disadvantages of them. This is the first review article to address a critical and exhaustive review of many different procedures to correct photon self-attenuation effects when using gamma-ray spectrometry, which can be of great interest for many research groups worldwide dedicated to measure natural and artificial radionuclides.

2. Materials: sample pretreatment, gamma detectors and geometries

2.1. Sample pretreatment

Before the measurement of solid samples, they need to be dried until constant weight using a temperature for which no decomposition of volatile compounds is produced, generally 60–70 °C is proper dryness temperature. This is really important in order to consider all the major elements that are present in the sample to obtain its mass attenuation coefficient.

When obtaining the sample mass attenuation coefficient, different multielement techniques such as XRF, ICP-MS/OES or XRD can be used. The XRF technique has several advantages versus other multielement techniques such as ICP-MS or ICP-OES since when using XRF, no digestion of the sample is needed that is it is a non-destructive technique (De Francesco et al., 2018). This is quite recommendable for samples that are quite complicated to be digested using, for example, digestion methods such as near to total dissolution using concentrated strong acids like HNO_3 (65% w./w.), HCl (37% w./w.), HF (30% w./w.) and $HClO_4$ (70% w./w.) (Liao et al., 2019; Karasaka, 2021). In the case of samples very complicated to be digested such as refractory materials, other digestion methods like alkali fusion are needed whose procedure is more complicated than near to total dissolution (Lei et al., 2024). Therefore, if sample digestion is not properly done, element concentrations can be quite lower than those really present in samples, making the sample mass attenuation coefficient obtention not proper. In addition, there are several elements such Ba that is usually quite insoluble. So, in the case that the sample contains a significant proportion of Ba, ICP-MS/OES is not a proper option for multielement analysis. Another advantage of XRF versus ICP-MS/OES is the possibility to obtain a chemical composition normalized at about 100% using semiquantitative standard analysis (OMNIAM, 2022) which is quite important when calculating the mass attenuation coefficient. In some cases, ICP-MS/OES is employed for obtention of the major element concentrations to calculate sample mass attenuation coefficient but this is not proper when sample chemical composition cannot be normalized at 100% only using oxygen, so if there is a relative high percentage of chemical element concentrations not considered to calculate sample mass attenuation coefficient, self-attenuation effect corrections can be unproperly addressed (Iuriana et al., 2018). A possible disadvantage of using XRF can be the self-attenuation effects related to photons emitted from electron deexcitations (Budak et al., 1999). So, as occurred for gamma photons in the case of gamma-ray spectrometry, the use of self-attenuation effect corrections for photons when using XRF is essential when the calibration and problem samples are very different regarding their chemical composition and apparent densities. When using XRD for very crystalline samples, it is also possible to obtain the concentrations of major elements through the different crystalline phases. However, for the great majority of the qualitative and quantitative analyses of the crystalline phases present in a sample, a previous knowledge of which chemical elements are present in the sample is required (DIFFRAC, 2016), so this technique is useful to obtain the mass attenuation coefficient in the cases of crystalline samples whose chemical composition are qualitatively known.

Another issue to be considered when applying the self-attenuation effect corrections is the homogeneity of both problem and calibration samples. Note that when using the mass attenuation coefficient for both problem and calibration samples, the same chemical composition is considered for the entire sample, so significant inhomogeneities are going to cause discrepancies regarding the self-attenuation effects for

photons emitted from the same sample layer considering trajectories parallel to the coaxial detector axis. Therefore, proper homogenization techniques as quartering are recommendable to employed (Civilbolg, 2015; Alakangas, 2015), which is especially true when the amount of samples is very high, for example, in the cases of mining wastes such as scales, flotation sludges or roasted ashes (Alakangas, 2015), where a significant amount of sample is needed to be taken in order to consider a representative sample.

Moreover, regarding the calibration and problem samples homogeneity, apart from the chemical composition issue discussed previously, it is very important to consider the homogeneity regarding sample compaction. When correcting self-attenuation effects, only a single apparent density is considered for the entire sample, so a proper sample compaction procedure must be employed. If significant inhomogeneities are present in the sample regarding its compaction level, the self-attenuation for photons emitted from the same sample layer, considering photon trajectories parallel to the coaxial or radial detector axis (for coaxial or well-type detectors), are going to be different depending on the apparent density present in each part of the sample.

In addition, another very important issue to address when carrying out self-attenuation corrections is the distribution of the sample inside the geometry employed. In the case of measuring granular solid samples, it is more recommendable to calibrate in efficiency also using granular solid samples instead of standard dissolutions since the possible porosities formed when compacting solid samples are not going to be considered using standard dissolutions (Ramos-Lerate et al., 1999).

2.2. Gamma detectors

Depending on the gamma detector type, the self-attenuation effect corrections are more or less employed. In the case of Ge detectors, for coaxial and well-type detectors, the self-attenuation effect corrections are usually employed even for non-extended range Ge detectors, that is, those whose detector window is composed of aluminum. Then, for scintillators such as $CeBr_3$(Cs) or NaI(Tl) whose energy resolutions are classified as medium and low, respectively, the self-attenuation effect corrections are usually neglected since only radionuclides whose gamma emission energies are relatively high, that is, generally energies higher than about 609 keV (^{214}Bi) can be relatively properly measured (Hasan et al., 2021). In the case of NaI(Tl) detectors, Chiozzi method is usually employed to calibrate in efficiency considering the interferences present for each region of interest (ROI). However, when using that method to obtain the *FEPE* for each ROI, the self-attenuation effect corrections are usually neglected, which can cause a relevant inaccuracy when obtaining the *FEPEs* since for energies higher than 609 keV, self-attenuation effects can also be relevant as previously explained in Introduction section. In the case of samples whose chemical compositions and apparent densities are very different from those related to the calibration sample, for example, when measuring a problem sample of uranite and calibration sample of water, f_a^{-1} can reach values about up to 1.5–2 for energies ranged from 609 keV to 1765 keV (^{214}Bi). Therefore, the non-use of self-attenuation effect corrections for those energies can cause very significant inaccuracies when obtaining the problem sample *FEPEs* where *FEPE* values can be deviated from corrected values about up to 50–100% for that energy range.

2.3. Geometries

In the case of the geometries that are usually employed in gamma-ray spectrometry, they are of polypropylene cylindrical type or characterized by having cylindrical such as Marinelli (Barba-Lobo et al., 2021a, 2021b, 2023b, 2024) which is really recommendable to maximize the geometrical efficiency, which is really recommendable for very low active samples such as waters or plants. However, in the case of Marinelli type, when using experimental methods for self-attenuation effect corrections, different approaches are needed as will be discussed in Section 3.1.1.2. Therefore, the main reason why cylindrical geometries are usually employed for gamma-ray spectrometry measurements is due to the relatively ease to fulfill the different conditions required when applying self-attenuation effect correction methods as will be discussed in Section 3. The different characteristic dimensions of the main geometries used for coaxial and well-type detectors are shown in Fig. 1. This figure is really useful for the comprehension of discussions carried out in Section 3.

3. Methodologies for self-attenuation corrections

3.1. Experimental methodologies

3.1.1. Coaxial detectors

3.1.1.1. Cylindrical geometries. In the case of coaxial detectors and cylindrical geometries (see Fig. 1), Cutshall model (Cutshall et al., 1983) is usually employed to correct self-attenuation effects using the following analytical function for f_a:

$$f_a = \frac{\eta_c \rho_c \left(1 - e^{-h\eta_p \rho_p}\right)}{\eta_p \rho_p \left(1 - e^{-h\eta_c \rho_c}\right)} \tag{2}$$

where the variables present in Eq. (2) were previously defined in Introduction section.

When using Cutshall model, different requirements are needed to be fulfilled in order to be possible to apply that method. One of them is the need for using cylindrical geometry, which is essential in order to consider only photons whose trajectories are parallel to coaxial detector axis. Then, the need to use the same thickness, h, for both calibration and problem samples. Regarding the sample radius, no dependence is considered which is consequence of another requirement that is the consideration of only photons whose trajectories are parallel to the coaxial detector axis, that is, no angular dependence is considered. This is the reason why only the sample thickness, h, is considered regarding geometrical conditions in Eq. (2). In addition, calibration and problem samples geometries must be the same.

One of the main advantages of these models is the relatively simplicity of the analytical function provided by Eq. (2) as well as the results are generally satisfactory for a wide energy range, from about 46 keV (^{210}Pb) to about 2615 keV (^{208}Tl), which can be proven for many different sample matrices and cylindrical geometries Barba-Lobo (2025).

Then, when the chemical composition and apparent density of the problem sample is quite different from those related to the calibration sample, the requirement of parallelism between the photon trajectory and coaxial detector axis is not properly fulfilled as can be shown in different studies (Barba-Lobo, 2025; Barba-Lobo and Bolívar, 2022). In the case of Barba-Lobo (2022), an upper limit value of 1.54 $cm^2\ g^{-1}$ was found for the problem sample mass attenuation coefficient at 63 keV (^{234}Th) for the proper application of this model, when using RGU-1 as calibration sample. An explanation to this effect can be related to the fact that when applying self-attenuation effect corrections for coaxial detectors and cylindrical geometries, an angular function depending on θ, where θ is the angle formed between the photon trajectory and coaxial detector axis, must be considered when calculating f_a for those cases. Another disadvantage of using this model is the non-fulfilling of that parallelism requirement when using very thin cylindrical geometries or thick geometries but considering high sample thicknesses. This is very consistent since for those cases, the probability of detecting a significant number of photons whose trajectories are not parallel to coaxial detector axis increases.

A possible solution to this problem is analyzed in previous studies (Barba-Lobo and Bolívar, 2022). When increasing the sample-detector distance, the solid angle sustained decreases, therefore θ is closer to 0. The main disadvantage of using this method is the considerable increase

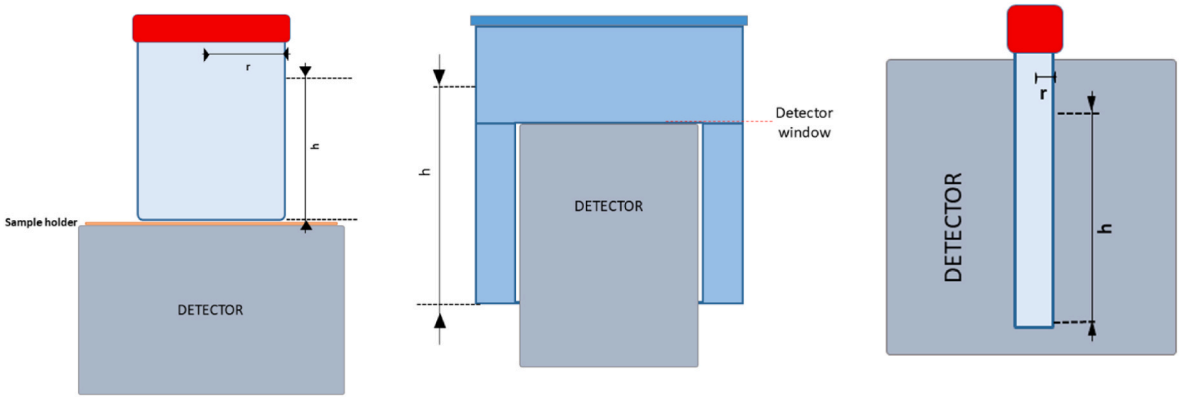

Fig. 1. Typical geometries (cylindrical, Marinelli and vial types) employed for coaxial and well-type detectors (on the left and center, and on the right, respectively), where h and r are the sample thickness and radius.

of the minimum detectable activity concentration since the *FEPE* significantly decreases when increasing the sample-detector distance. Therefore, this is a relevant issue for samples whose radionuclide activities are relatively low.

3.1.1.2. Marinelli geometry. Then, when using Marinelli geometries instead of cylindrical ones for coaxial detectors (see Fig. 1), it is possible to maximize the *FEPE* for each specific energy since the geometrical efficiency is maximized, and therefore, also the full-energy peak efficiency. When using Marinelli geometry, different maximum volumes can be considered for this geometry type such as 0.5 L, 1 L or 5 L. Therefore, this geometry type is useful when having a considerable amount of sample since if the sample thickness is not enough upper the detector window, the *FEPE* is going to be quite low since it is very complicated that photons emitted from the sample can be detected (Barba-Lobo et al., 2024). This is reason why this geometry type is usually employed for liquid samples since for the great majority of the cases, relatively high amounts of sample are available and it is relatively easy to reach the minimum detectable activity concentrations when using this geometry even for relatively low active samples such as waters. When using this geometry type for solid samples, a very proper homogenization procedure is needed to carry out, as explained in Section 2.1, because of the high amount of sample required using this geometry type.

In the case of using Marinelli geometry, an approximation for f_a can be written as follows (Modarresi et al., 2018):

$$f_a = \frac{1 - e^{-\eta_p \rho_p h}}{\eta_p \rho_p h} \tag{3}$$

where the variables involved in Eq. (3) were previously defined.

Eq. (3) is clearly a version of Eq. (2), specifically in the case of carrying out the self-attenuation effect corrections regarding vacuum case, since as can be seen in Eq. (3), no consideration of the variables corresponding to the calibration sample. Eq. (3) can be a proper approximation for f_a when using Marinelli geometry but for the part upper detector window since as can be seen in Fig. 1, it can be considered as cylindrical geometry. The problem of using this f_a function for this geometry is related to the part under detector window which cannot be considered as a cylindrical geometry. For this reason, there is no general equation for f_a when using this geometry type. Therefore, f_a must be obtained for each specific coaxial detector using experimental methodologies.

Considering that previously discussed, different methods are developed. One of them is using a semiempirical function for f_a depending on the sample mass attenuation coefficient and thickness (Modarresi et al., 2016). In this case, the problem is that when obtaining f_a, it is also necessary to use Eq. (3). Ther, using that methodology, there is an that allows to obtain an analytical expression for f_a for the different self-attenuation effects present between two different samples, let us call 1 and 2, characterized by having different mass attenuation coefficient, η_1 and η_2, and thickness, h_1 and h_2. Therefore, f_a can be generally written for two any samples as follows:

$$f_a = \frac{\varepsilon_1(\eta_1, h_1)}{\varepsilon_2(\eta_2, h_2)} = \frac{\varepsilon_{01}(\eta_1 = 0, h_1)\, f_{a1}(\eta_1, h_1)}{\varepsilon_{02}(\eta_2 = 0, h_2)\, f_{a2}(\eta_2, h_2)} \tag{4}$$

where ε_1 and ε_2 are the *FEPEs* obtained for samples 1 and 2, ε_{01} and ε_{02} are the *FEPEs* obtained at h_1 and h_2 for vacuum case, and $f_{a1}(\eta_1, h_1)$ and $f_{a2}(\eta_2, h_2)$ their respective self-attenuation effect corrections.

In addition, $f_{ai}(\eta_i, h_i)$ can be expressed as the following ratio:

$$f_{ai} = \frac{Eq.\ 3\ (for\ \eta_i, h_i)}{Eq.\ 3\ (for\ \eta_i = 0, h_i)} \tag{5}$$

Therefore, the clear problem of applying the previous model is the need to use Eq. (3) for the f_{ai} obtention, since Eq. (3) is only proper to be applied for cylindrical geometries, so approaches relatively acceptable are carried out when obtaining f_a. After obtaining a fit function for f_{ai} versus η_i for each fixed h_i, it is possible to obtain the *FEPE* for vacuum case, ε_{0i}. Once the *FEPEs* are calculated, which is possible using the following equation:

$$\varepsilon_i = \frac{N}{P_\gamma a_i m_i t} \tag{6}$$

where N is the net counts of each full-energy peak. P_γ is the gamma emission probability, a_i is the concentration of each radionuclide in the sample i, m_i is the sample mass and t is the counting time.

One of the main advantages of using the previous methodology is the possibility to carry out the self-attenuation effects considering different thickness for the two samples considered for their analysis. This is an advantage compared to the model discussed in previous Section.

The main disadvantage of calibrating in efficiency varying h using solid samples for this geometry type is the need to properly compact the calibration sample for each case in order to properly apply self-attenuation effect corrections as explained in Section 2.1. Another option to calibrate in efficiency using this geometry type is varying the calibration sample mass attenuation coefficient if always desiring to use the same h, where this efficiency calibration is carried out fixing E_γ, therefore ε_0 can also be obtained as a function of E_γ. The main disadvantage of this another option is needed to properly mix different calibration sample matrices to avoid possible inhomogeneities for each mix and therefore, to properly use the calibration sample mass attenuation coefficient at each energy for the f_{ai} calculation in order to obtain ε_0 for each case. This is more complicated when using higher amounts of samples as explained in Section 2.1.

3.1.2. Well-type detectors

When using well-type detectors, cylindrical vials are usually employed and usually using Appleby model (Appleby et al., 1992) in order to correct self-attenuation effects. For this case, f_a function can be written as follows:

$$f_a = 2\exp(-kx^2)\left[(kx^2)^{-1}\sinh(kx^2) - (kx^2)^{-2}\left(\cosh(kx^2)-1\right)\right] \quad (7)$$

where $x^2 = \eta_p m_p$, m_p is the problem sample mass, k is the geometric parameter characterizing the dimensions of the sample, which is given by $k = (\pi r_p h_p)^{-1}$.

Note that in Eq. (7), analogously to Marinelli geometry, there is no presence of variables related to the calibration sample which is due to the self-attenuation effect corrections are carried out regarding vacuum case as explained for Marinelli geometry in Section 3.1.1.2. Therefore, after obtaining ε_c using Eq. (6) fixing E_γ and varying h or in the opposite case, ε_0 can be obtained as

$$\varepsilon_0 = \varepsilon_c \Big/ f_a = \frac{\varepsilon_c}{Eq.\ 7\ (for\ calibration\ sample)} \quad (8)$$

In addition, an analytical function can be obtained for ε_0 when fitting ε_0 versus E_γ or h in the case of calibrating in efficiency varying h and fixing E_γ or in the opposite case, respectively. The main problem of carrying out this type of methodology to obtain ε_0 is the need to consider Eq. (7) as valid for the calibration samples employed. So, in the case that ε_0 is not properly obtained for certain energies due to an unproper correction through Eq. (7), this is going to affect all problem sample *FEPE* values obtained at those energies as can be seen in Eq. (9).

Therefore, the problem sample *FEPE* can be written as follows:

$$\varepsilon = \varepsilon_0 f_a \quad (9)$$

Therefore, for this case is also needed to obtain the *FEPE* for vacuum case, as occurred in Section 3.1.1.2. In this case, since the amounts of sample employed for its measurements using well-type detectors are relatively low, for example, 5–10 g for 5 mL vials, the option of carrying out the efficiency calibration varying the calibration sample mass attenuation coefficient is a proper methodology which was deeply developed by Barba-Lobo et al. (2021a).

Then, note that Eq. (7) is quite different from Eqs. (2) and (3), which is due to in this case, the self-attenuation effect corrections are carried out considering the radial geometry axis, not the coaxial axis as previously occurred in Section 3.1.1 for coaxial detectors. However, as occurred for coaxial detectors, no angular dependence is considered when carrying the self-attenuation corrections using Eq. (7). This is due to when applying this method to correct self-attenuation effects, an essential requirement must be fulfilled which is the need for the emitted photon trajectory to be parallel to the radial axis of the cylindrical geometry. Another requirement is the need to use the same sample thickness and radius as well as same geometry when calculating both *FEPEs*, that is, ε and ε_0.

Therefore, as previously occurred for coaxial detectors, the self-attenuation effect correction using Eq. (7) has a relatively limited application range, having proved that for problem sample whose apparent density and chemical composition are very different from those related to the calibration sample, the previous requirement is not properly fulfilled as clearly proven by Barba-Lobo et al. (2021a), where an upper limit value of η was found to be 1.57 $cm^2\ g^{-1}$ at 63 keV (^{234}Th) for proper application of this model, when using vials whose radius is 0.69 cm and sample thickness of 3.5 cm. The main disadvantage of using well-type detectors is that is not possible to correct the previous issue varying the sample-detector distance as carrying out for coaxial detectors, see Section 3.1.1.1. However, reducing the problem sample thickness is possible to reduce the self-attenuation effect which can make possible to properly correct self-attenuation effects using Eq. (7). This is possible if the efficiency calibration is carried out varying the calibration sample thickness. In addition, the well-type detectors are characterized by having a *FEPE* for each specific energy quite higher compared to that related to the great majority of coaxial detectors, which is mainly due to their higher geometrical efficiency, therefore the minimum detectable activity is very probably to be properly reached even in cases for which the problem sample thickness needs to be reduced as previously discussed.

3.2. Simulated methodologies

3.2.1. LabSOCS

When using LabSOCS software to obtain the problem sample *FEPE* (Barba-Lobo, 2025; Barba-Lobo et al., 2023b, 2024), where this simulation code is usually employed for Mirion gamma detectors, it is necessary to previously design the geometry dimensions and shape using Beaker editor which is a module of Geometry Composer (Canberra Industries, 2004, 2012). This design of the geometry must be carried out manually, so depending on the geometry complexity, this can be a relatively complicated and time-consuming task. When using Beaker editor, it is also needed to design the inner contour, which can sometimes be a complicated task depending on the geometry contour hardness since it is usually needed to cut the geometry into different pieces for a proper design of the geometry contour. However, using Beaker editor, it is possible to accurately reproduce the employed geometry which is quite needed in order to properly obtain the *FEPEs*. The geometry generated using Beaker editor can be saved as a.BKR file.

Then, for that.BKR file, it is needed to specify the problem sample chemical composition and apparent density as well as its thickness using Geometry Composer, which can be saved as a.geo file. If another problem sample thickness is desired to be used for the same previous geometry, it can be easily inserted using the previous.geo file. In the case of the problem sample mass attenuation coefficient, it is considered included in the.par file after generating that.geo file, where.par file is one of the file needed to specify when carrying out simulations using LabSOCS, where this file is only related to a specific detector. Using that. geo file, it is possible to create a *FEPE* file, .ecc file, for problem sample.

One of the main disadvantages of using LabSOCS to obtain the *FEPEs* for the problem samples compared to experimental methods, see Section 3.1, is the limitation that LabSOCS has regarding the number of major elements that can be specified, where nine is the upper limit (Barba-Lobo, 2025). This can suppose an inconvenient when using samples which contain a long number of major elements whose concentrations are relatively high, and therefore significantly contributing to the problem sample mass attenuation coefficient as can be seen in previous studies.

For a wide range of sample matrices, apparent densities, geometries and energies, the robustness of LabSOCS calculating the *FEPEs* for problem samples is deeply demonstrated (Barba-Lobo, 2025; Barba--Lobo et al., 2023b, 2024), which is one of the main advantages of using this simulation code compared to experimental methods detailed in Section 3.1. In the case of using same geometry (like Fig. 1 on left) and sample thickness than those used by Barba-Lobo (2022), the robustness of LabSOCS calculating *FEPE* for problem sample is much higher than that obtained when using Eq. (2) (Section 3.1.1) as proven by Barba--Lobo et al. (2023b), where satisfactory results were obtained for η up to 2.73 $cm^2\ g^{-1}$ at 63 keV. This is mainly due to many different angles between emitted photon trajectories and coaxial or radial detector axis are considered when using this simulation code, therefore its applicability range is much wider than experimental methodologies.

Other main advantage of using this simulation code is the possibility to be applied to be applied to many geometry types such as cylindrical, Marinelli, rectangular and spherical type, as well as any other geometry type which has cylindrical symmetry. Therefore, it is not needed to employ different self-attenuation methods depending on the geometry or detector type as occurred when using experimental methods. When using this simulation code, the *FEPE* is directly obtained for the problem

sample, which makes it unnecessary to carry out a *FEPE* transformation as occurred when using experimental methodologies to correct self-attenuation effects.

Another issue to discuss is the non-need to experimentally measure the problem samples in order to obtain their *FEPEs*. This feature has advantages and disadvantages versus experimental procedures. One of the main advantages is the non-need for sample preparation avoiding possible inhomogeneities for chemical composition and for apparent density during compaction procedure. However, the usage of this procedure to obtain *FEPEs* can sometimes be not enough realistic when reproducing real compaction and sample porosity conditions that are present when experimentally measuring problem samples in order to calculate activity concentrations using LabSOCS which is a possible disadvantage versus experimental methodologies.

3.2.2. EFFTRAN

When using EFFTRAN in order to calculate the *FEPEs* for problem samples (Vidmar et al., 2011), an Excel file is employed for the simulations, so it is open download, this is one advantage versus LabSOCS for which license is required. When using EFFTRAN, different information about the detector parameters, calibration and problem samples regarding their chemical compositions, mass attenuation coefficients, apparent densities and dimensions are needed to be specified. In the case of the detector parameters, there is a specific sheet in the Excel file where they can be specified. Then, regarding the characteristics of the calibration and problem samples as well as for their respective containers, there is another specific sheet to be inserted. In the case of calibration and problem samples' mass attenuation coefficients, they are taken from XCOM database (NIST, 2006). Finally, there is a third sheet where the *FEPE* for calibration sample can be obtained where it is necessary to specify the.CAL or.EFT file generated using Genie 2000 or Gamma Vision, respectively, after experimentally measured the calibration sample. After obtaining the *FEPEs* for the calibration sample, it is possible to transform the *FEPEs* to problem sample ones.

Therefore, in the case of this simulation code, several advantages and disadvantages can be observed compared to LabSOCS. In the case of the geometry design, when using EFFTRAN it is not possible to detail any kind of imperfections present in them, where they are needed to be considered as completely cylindrical. In addition, it is not possible to consider another volume geometry type apart from cylindrical type. These are clear disadvantages compared to LabSOCS.

When obtaining the *FEPEs* for the problem sample, an experimental measurement for calibration sample considering a specific sample thickness is required in order to generate the.CAL or.EFT file that is needed to obtain the *FEPEs* for calibration sample. This has clear advantages and disadvantages versus LabSOCS. In the case of the sample preparation and experimental measurements to obtain the *FEPEs*, they are not required when using LabSOCS.

In addition, another point to be considered is the need to carry out the preparation and measurement for each sample thickness selected. This has clear disadvantages versus LabSOCS. Then, as discussed in Section 3.2.1, the *FEPE* obtention using LabSOCS can sometimes be not enough realistic when not considering possible porosities and other physical features of the problem samples, where this problem is solved using EFFTRAN since experimental measurements are required to obtain *FEPEs*. When obtaining the *FEPEs* for calibration and problem samples, there is no limit regarding the major elements that can be specified for each sample, so this is a clear advantage versus LabSOCS.

Then, regarding the different crystal types that can be considered when using EFFTRAN, they can be of Ge, NaI, $LaBr_3$, CZT, CLYC and CsI types. In the case of LabSOCS, it is only possible to simulate the problem sample *FEPEs* for Ge, NaI and $LaBr_3$ types, although in the case of Ge detectors, they can be of both types coaxial and well-type detectors.

Another issue to discuss is the obtention of *FEPEs* for specific energies when using EFFTRAN, where no additional energies can be inserted in Excel file. This makes necessary to use a fit *FEPE* function versus energy for both calibration and problem samples which can be an inconvenient due to possible deviations between the experimental and fitted *FEPEs* causing inaccuracies in the *FEPE* calculation for any other energy not considered in the list specified in Excel file. In addition, the use of a *FEPE* function can also be a problem for energies affected due to true coincidence summing (TCS) effects if TCS are not properly corrected.

3.2.3. DETEFF

In the case of DETEFF (Diaz and Vargas, 2010; Díaz and Vargas, 2008), it is a simulation code based on Monte Carlo which is written in Borland Delphi 3 and running using Windows platform, so when using DETEFF, the computational cost is much less than using Monte Carlo code.

In the case of DETEFF, as occurred when using EFFTRAN, there is a section where the detector parameters must be specified, which need to be interested manually in the case of DETEFF while when using EFFTRAN, it is possible to inserted automatically using Excel macros. When using DETEFF, it is also possible specify the crystal type where the possible options are Ge, NaI, CsI and Si, therefore it is more limited than EFFTRAN regarding this feature.

Regarding the different geometry types possible to be considered using DETEFF, they are cylindrical, Marinelli and rectangular types, so it is improved compared to EFFTRAN regarding the possible geometry types that can be selected. However, as occurred when using EFFTRAN, it is not possible to modify manually the geometry contour to consider imperfections. Therefore, this is a disadvantage versus LabSOCS as well as when using LabSOCS many more geometry types can be addressed since they can be manually designed using Beaker editor option.

Then, regarding the *FEPE* obtention for problem sample, it can be directly obtained for problem sample where there is no need to transform the *FEPE* from calibration sample to problem sample as occurred when using LabSOCS. Therefore, this is an advantage versus EFFTRAN since no analysis is required regarding calibration sample. In the case of the database used for mass attenuation coefficient, they are taken from XCOM as occurred when using EFFTRAN, where a fit function is employed to the tabulated sample mass attenuation in order to obtain it for any energy. In this case, there is no limitation regarding the number of major elements that can be specified for each sample, so this is an advantage versus LabSOCS.

In addition, when obtaining the *FEPE* using DETEFF, no experimental measurement is required, so much less time-consuming than experimental methodologies or EFFTRAN. However, as discussed in Section 3.2.1, it is possible for solid samples not to reproduce in an enough realistic way the possible porosities formed inside the container when compacting the problem sample. Then, the *FEPE* can be obtained for each specific energy when using DETEFF, where no *FEPE* fit versus energy is required. This is a clear advantage versus EFFTRAN.

3.2.4. PENELOPE

When using PENELOPE (Guerra J et al., 2015, 2018), it is a simulation code based on Monte Carlo simulation, where subroutines written in FORTRAN, allowing to carry out Monte Carlo simulations of coupled electron–photon transport for energies ranged from about 100 eV to 1 GeV. When using PENELOPE, from the compilation of PENELOPE using a FORTRAN subroutine, it is possible to create an executable file which is employed to carry out the simulations as well as to specify the parameters of the detector.

In addition, it is also necessary to optimize the computational model of the detector to carry out its characterization, where different algorithms such as DE algorithm can be used. Therefore, it is possible to generate a file including the simulated gamma spectrum, which is needed to calculate the *FEPEs*. In the case of the optimization process, this is required in order to know all the detector parameters (p_r) needed to obtain the simulated *FEPEs* such as dead layer thickness. When, carrying out this process, minimum and maximum values (p_r^{min}, p_r^{max}) for each of those detector parameters are needed to be specified in order to

find optimal solution for each of them, where this process was previously validated for coaxial and well-type Ge detectors. For *FEPE* obtention using this simulation code, relative squared differences between experimental *FEPEs* obtained using Eq. (4) for a calibration sample and those simulated through this simulation code are minimized using the following function (Guerra et al., 2018; Guerra et al., 2015)):

$$F(p_r) = \sum_i \left(\frac{\varepsilon_{PENELOPE}(p_r, E_{\gamma_i}) - \varepsilon_c(E_{\gamma_i})}{\varepsilon_c(E_{\gamma_i})} \right)^2 \quad (8)$$

where $\varepsilon_{PENELOPE}(p_r, E_{\gamma_i})$ and $\varepsilon_c(E_{\gamma_i})$ are the *FEPEs* at each E_γ obtained after optimization process using PENELOPE and those obtained experimentally using Eq. (4) for a calibration sample, so these *FEPEs* are needed as reference values in order to proceed with the optimization process.

Note that the previous optimization process is only needed if detector characterization is carried out using this simulation code which is completely optional since it is possible to be characterized using through different companies but this process is usually expensive and takes a relatively long time avoiding the usage of the detector during that time interval. However, when carrying out the detector characterization using that optimization procedure, it is needed the preparation and experimental measurements of calibrations samples which can be time-consuming depending on the case.

Therefore, the use of this simulation has clear advantages and disadvantages versus the previous methodologies. In the case of the process to obtain the *FEPEs*, as can clearly be seen this process is quite much tedious compared to other simulations such as LabSOCS, EFFTRAN or DETEFF since when using PENELOPE, it is necessary to write all the code lines needed to generate the simulated *FEPEs*.

Then, regarding the different geometry types that can be considered when using this simulation code, for cylindrical geometries, it is possible to select, for example, pencyl.f as subroutine in FORTRAN since this option is for geometries characterized by having cylindrical symmetry. In addition, for other cases, geometrical information as well as the problem sample chemical composition and apparent density are needed to be specified as an input file. In the case of the problem sample mass attenuation coefficient, data from XCOM database are considered when carrying out the simulations to obtain the problem sample *FEPEs*. However, there is no geometry editor as occurred when using Beaker editor in the of LabSOCS, which makes not possible to detail in depth dimensions of the geometries and design a wide range of geometries. Therefore, this is a disadvantage compared to LabSOCS. In this case, as occurred when using LabSOCS and DETEFF, no need for the calibration sample *FEPE* is needed in order to obtain the problem sample *FEPE*, so this is a clear advantage versus EFFTRAN since no radioactive and multielement characterization of calibration sample is needed.

Regarding the detector type that is possible to select in order to carry out simulations using this simulation code, it is possible to observe a clear robustness since it can be applied to coaxial and well-type detectors, since using the previous optimization process, the detector characterization can be carried out for a wide range of detector types.

3.2.5. Geant4

In the case of Geant4 (Dziri et al., 2012; Quintana and Montes, 201), it is an object-oriented toolkit utilizing C++ programming language, which allows to simulate particle interactions in high-energy experiments. Geant4 is based on Monte Carlo code and theoretical models to simulate the entire process of passage and interaction of particles with matter, where the energy range possible to be analyzed is about 250 eV-100 GeV. The upper energy limit is two orders of magnitude higher than that allowed when using PENELOPE, but this is not a problem when using gamma-ray spectrometry since the great majority of gamma emitters have gamma emission energies up to about 2615 keV (^{208}Tl). In the case of the formation of the gamma spectrum, all relevant physical processes and interactions are considered when simulating using this code, so no approximations are made for Monte Carlo calculations, achieving generally uncertainties less than 1% when considering about one million of events for each simulation. This is one of the main reasons of the high computational cost when using Geant4 compared to, for example, DETEFF for which approaches are considered to reduce that computational cost. When carrying out simulations using Gean4, the physical processes must be included as an input file.

Using this simulation code, it is needed to consider different features such as the system geometry and materials, involved particles and physical processes, primary particle generations, passage of particle through materials and their interactions with matter, and detector response. To carry out simulations using Geant4, it is usually needed to define three user classes for compulsory: DetectorConstruction.cc, PhysicsList.cc, and PrimaryGeneratorAction.cc (Geant4 Collaboration, 2016).

When carrying out the compiling user classes, they are directly linked to the Geant4 library results in a detector executable file. The code directly generated files in ROOT format. In the case of particle trajectory and geometry visualization, it can be carried out using, for example, Wired and Dawn visualization tools, which are coupled with Geant4.

When simulating the full-energy peak efficiency for any problem sample using this simulation code, the different interactions of gamma photons with matter are considered: photoelectric effect, Compton scattering, Rayleigh scattering and pair production. A subsequent analysis enables the building of a simulated photopeak when the photons fully deposit their energy. The problem of simulating the full-energy peak using Geant4 is that it does not consider the detector energy resolution, that is, the full width at half maximum (FWHM) is zero for each full-energy peak, so they are considered as lines in the gamma spectrum, which is not so realistic because the FWHM is usually higher than 1–2 keV, where FWHM = 1–2 keV are typical values for Ge detectors.

However, it is possible to solve the previous FWHM issue using a Gaussian broadening function which is written as follows:

$$FWHM = a + bE_\gamma^{-1/2} \quad (9)$$

where a and b are related to electronic background of acquisition chain and intrinsic properties of detector crystal, respectively.

However, the approach for FWHM using Eq. (9) can be not enough realistic depending on the case since the distribution of registered events for each full-energy peak can be relatively different from a Gaussian distribution. Indeed, in the case of using Genie 2000; Canberra Industries (2012), wh) for experimental methodologies to calculate the *FEPEs*, see Section 3.1, there is a supplementary option that can be installed in Genie (2000), which is Interactive peak fit. Using this supplement, it is possible to consider different statistical distributions for each single full-energy peak such Gaussian distribution but with low-energy tail which makes the net count calculation more accurate.

In the case of using Geant4, using the theoretical definition of the *FEPE,* it can be obtained as follows:

$$\varepsilon = N/N_{des} \quad (10)$$

where N is previously defined and N_{des} is the number of disintegrations that occurred at the energy of interest, where the units of ε are usually expressed as cps/dps, that is, counts per second/disintegration per second, where N can be obtained through the simulated gamma spectrum and N_{des} is obviously known since is needed to be specified when carrying out each simulation.

Therefore, different advantages and disadvantages can be found when calculating the *FEPE* for any problem sample using this simulation code. As occurred when using PENELOPE, the performance of the problem sample *FEPE* calculation can be quite tedious considering the numerous code lines to be written as well as the large number of files required to carry out each simulation. These are clear disadvantages

compared to the other simulation codes previously discussed. In addition, the computational cost is another issue to be considered. When carrying out *FEPE* simulations using Geant4, about 10^6-10^9 of events are considered for each simulation in order to obtain statistical uncertainties relatively, less than 1%, for the net number of counts of each full-energy peak.

In the case of using this simulation code for *FEPE* obtention, no transformation from the calibration sample *FEPE* to the problem sample *FEPE* is required, so this is a clear advantage versus experimental methodologies and EFFTRAN. For the problem sample *FEPE* obtention, no experimental measurement is required, so this is another advantage versus experimental methodologies and EFFTRAN. However, as discussed in previous sections, see Section 3.2.2, this has also disadvantages regarding the realism of the simulated data. As previously discussed in the case of Geant4, the FWHM is not considered when obtaining the simulated gamma spectrum. However, different solutions are possible to be performed as previously discussed.

Regarding the different geometries possible to considered using this simulation code, it is possible to address different types of regular shapes such as cylindrical, rectangular and spherical types. However, it is not possible to manually design the geometry as occurred when using LabSOCS, where the only requirement when using Beaker editor is the need for cylindrical symmetry.

In the case of the different detector types possible to be considered when simulating *FEPE* using this simulation code, there is no restriction since specifying the detector dimensions and materials as an input file when carrying out the simulations, all those characteristics can be considered for both coaxial and well-type detectors. This is an advantage versus EFFTRAN or DETEFF.

Regarding the applicability range for this simulation code to obtain the problem sample *FEPE*, it is proven that it is possible to consider a wide range of sample chemical compositions and apparent densities as well as energies. This is possible due to there is no restriction regarding the different angles that the emitted photons can form regarding the coaxial or radial detector axis in the case of coaxial or well-type detectors, respectively. This is a clear advantage versus experimental methodologies.

3.3. Comparison among FEPEs obtained using experimental and simulated methodologies

3.3.1. Geant4 – LabSOCS – EFFTRAN

In the case of the simulated methodologies regarding LabSOCS, EFFTRAN and Geant4, it is possible to find different comparisons related to concentrations of radionuclides obtained for a wide range of sample matrices using each previous simulation code. As can be seen in Table 1, concentrations of ^{238}U and ^{235}U were obtained for a U sample whose apparent density was of 0.83 g cm^{-3}. The concentrations obtained using each code were statistically compatible with average values obtained considering the concentration values obtained at each energy. However, in the case of EFFTRAN, it is possible to observe a clear underestimation of concentration of ^{238}U at 63 keV, where a relative difference of 6% was obtained.

Then, for these same simulation codes, another comparison can be seen in Table 2 where same radionuclides were determined using same previous energies where the apparent density was changed to 2.21 g cm^{-3}. Analogously to previous case, concentrations were statistically compatible with average values, but again a clear underestimation of ^{238}U at 63 keV using EFFTRAN was obtained, where a relative difference of 6% was again obtained which shows a clear systematicity at that energy.

Further comparisons can be observed in the case of Geant4 – EFFTRAN, which can be seen in Tables 3 and 4. When using UO_2 sample (see Table 3), it is possible to observe again a clear difference between Geant4 and EFFTRAN at 63 keV, where a relative difference of 10% was obtained. When using RGU-1 sample (see Table 4), a significant difference can be seen at 1001 keV, obtaining a relative difference of 10%.

Table 1
Comparison between LabSOCS, EFFTRAN and Geant4 using U sample whose apparent density is 0.83 g cm^{-3} (Vraničar et al., 2022).

Software	RN	Energy (keV)	Concentration (MBq kg^{-1})	Average concentration (MBq kg^{-1})
LabSOCS	^{238}U	63.3 (via ^{234}Th)	3.56 ± 0.19	3.50 ± 0.11 (63 keV)
		1001.03 (via ^{234m}Pa)	3.59 ± .0.20	3.55 ± 0.06 (1001 keV)
	^{235}U	143.8	0.160 ± 0.010	0.163 ± 0.003 (144 keV)
		163.3	0.160 ± 0.010	0.166 ± 0.003 (163 keV)
		185.7	0.170 ± 0.010	0.175 ± 0.003 (186 keV)
EFFTRAN	^{238}U	63.3 (via ^{234}Th)	3.30 ± 0.19	
		1001.03 (via ^{234m}Pa)	3.44 ± 0.20	
	^{235}U	143.8	0.160 ± 0.010	
		163.3	0.170 ± 0.010	
		185.7	0.180 ± 0.010	
Geant4	^{238}U	63.3 (via ^{234}Th)	3.65 ± 0.18	
		1001.03 (via ^{234m}Pa)	3.63 ± 0.21	
	^{235}U	143.8	0.170 ± 0.010	
		163.3	0.170 ± 0.010	
		185.7	0.180 ± 0.010	

Table 2
Comparison between LabSOCS, EFFTRAN and Geant4 using U sample whose apparent density is 2.21 g cm^{-3} (Vraničar et al., 2022).

Software	RN	Energy (keV)	Concentration (MBq kg^{-1})	Average concentration (MBq kg^{-1})
LabSOCS	^{238}U	63.3 (via ^{234}Th)	6.6 ± 0.4	6.0 ± 0.3 (63 keV)
				6.2 ± 0.2 (1001 keV)
		1001.03 (via ^{234m}Pa)	6.6 ± 0.4	0.307 ± 0.017 (144 keV)
	^{235}U	143.8	0.32 ± 0.02	0.303 ± 0.003 (163 keV)
		163.3	0.31 ± 0.02	0.305 ± 0.003 (186 keV)
		185.7	0.32 ± 0.02	
EFFTRAN	^{238}U	63.3 (via ^{234}Th)	5.4 ± 0.3	
		1001.03 (via ^{234m}Pa)	5.8 ± 0.4	
	^{235}U	143.8	0.29 ± 0.02	
		163.3	0.30 ± 0.02	
		185.7	0.30 ± 0.02	
Geant4	^{238}U	63.3 (via ^{234}Th)	6.1 ± 0.4	
		1001.03 (via ^{234m}Pa)	6.2 ± 0.4	
	^{235}U	143.8	0.29 ± 0.02	
		163.3	0.29 ± .0.02	
		185.7	0.30 ± 0.02	

3.3.2. DETEFF – experiment

In the case of DETEFF code, a comparison with experimental methods based on Eq. (1) can be shown in Table 5, using a liquid sample containing artificial radionuclides. Relative differences were ranged from −2.93% to 3.32%, so no significant differences are obtained for that case.

Table 3
Comparison between EFFTRAN and Geant4 using UO_2 sample whose apparent density is 10.96 g cm^{-3} (Vraničar et al., 2021).

Software	RN	Energy (keV)	Concentration (MBq kg^{-1})
EFFTRAN	^{238}U	63.3 (via ^{234}Th)	3.56 ± 0.17
		1001.03 (via ^{234m}Pa)	5.68 ± 0.24
	^{235}U	143.8	0.233 ± 0.014
		163.3	0.245 ± 0.016
Geant4	^{238}U	63.3 (via ^{234}Th)	3.94 ± 0.21
		1001.03 (via ^{234m}Pa)	5.79 ± 0.87
	^{235}U	143.8	0.213 ± 0.014
		163.3	0.219 ± 0.014

Table 4
Comparison between EFFTRAN and Geant4 using RGU-1 sample whose apparent density is 1.23 g cm^{-3} (Vraničar et al., 2021).

Software	RN	Energy (keV)	Concentration (kBq kg^{-1})
EFFTRAN	^{238}U	63.3 (via ^{234}Th)	5.17 ± 0.24
		1001.03 (via ^{234m}Pa)	5.2 ± 0.3
	^{235}U	143.8	0.242 ± 0.019
		163.3	0.249 ± 0.021
Geant4	^{238}U	63.3 (via ^{234}Th)	5.2 ± 0.3
		1001.03 (via ^{234m}Pa)	5.8 ± 0.8
	^{235}U	143.8	0.193 ± 0.018
		163.3	0.204 ± 0.015

Table 5
Comparison between DETEFF and experimental methods to obtain *FEPEs* using liquid sample for a 250 mL Marinelli. (Díaz and Vargas, 2008).

RN	Energy (keV)	Deviation (%)
^{241}Am	59.54	−2.93
^{109}Cd	88.03	2.88
^{57}Co	122.06	2.35
^{139}Ce	165.86	0.35
^{85}Sr	514.01	−0.94
^{137}Cs	661.66	0.35
^{85}Sr	898.04	1.99
^{60}Co	1173.5	1.56
^{60}Co	1332	1.17
^{88}Y	1883	3.32

3.3.3. *Penelopè – experiment*

For that comparison shown in Table 6, dissolution and silica samples were used. As can be seen, relative differences between experimental and simulated *FEPEs* were not significant which were ranged from −0.86% to 2.84% and from −3.00% to 1.23%.

4. Conclusions

This is the first review study where an exhaustive critical review has been carried out about many different experimental and simulated methodologies usually employed to correct self-attenuation effects in gamma-ray spectrometry using coaxial and well-type detectors. For this, a comprehensive comparison has been carried out among the different methodologies discussing in depth the advantages and disadvantages of them as well as discussing different proposals to improve them. In addition, the previous steps to the self-attenuation effect corrections using each methodology such as sample pretreatments, and gamma detectors and geometries employed, were also discussed in depth in order to establish proper procedures and recommendations to be carried out.

Table 6
Comparison between PENELOPE and experimental methods to obtain *FEPEs*. (Jurado Vargas and Guerra, 2006).

Energy (keV)	$Deviation_{disolution}$ (%)	$Deviation_{silica}$ (%)
60	−0.86	−3.00
80	1.83	1.23
100	0.91	−0.14
250	1.40	−0. 3
500.0	−0.83	−1.34
1000	1.20	0.33
1500	1.15	0.120
2000	2.84	−0.85

From this review study, different main conclusions can be extracted.

1. In the case of the pretreatment employed for samples, a very proper homogenization and compaction procedures need to be applied in order to use reliable values for the sample mass attenuation coefficient and apparent densities for the self-attenuation effect corrections. In addition, proper multielement techniques need to be used depending on the sample, where a proper measurement of major elements is essential in order to calculate sample mass attenuation coefficients.
2. Gamma detectors such as Ge, NaI, CsI, $LaBr_3$ and $CeBr_3$ are usually employed for gamma-ray spectrometry. However, self-attenuation effect corrections are usually employed only for Ge detectors, and being not considered for the great majority of the scintillators due to only gamma emitters at relatively high energies can be properly measured. This can be an improper decision in the case of calibration and problem samples very different regarding their chemical composition and apparent densities.
3. In the case of experimental methodologies to correct self-attenuation effects, for coaxial and well-type detectors Cutshall and Appleby models are usually employed, respectively, when using cylindrical geometries. However, their applicability ranges are relatively limited regarding the possible problem sample chemical compositions and apparent densities to be addressed depending on the calibration sample selected. Therefore, it is really recommendable to properly test their validity depending on the case. When using Marinelli geometry, no general analytical function is possible to be obtained for the self-attenuation effect correction, f_a, making it necessary to obtain a specific semiempirical function for f_a for each specific detector. For this, different approaches need to be carried out which can be sometimes unacceptable.
4. For simulated methods, LabSOCS, EFFTRAN, DETEFF, PENELOPE and Geant4 are usually used to obtain the problem sample *FEPEs*.
   - 4.1 When using LabSOCS, the main advantage versus other simulation codes is the possibility to detailly design the geometry contour for inner and outer surfaces. This makes it possible to precisely consider geometrical conditions avoiding reducing inaccuracies when obtaining the *FEPE* due to geometrical efficiency. However, LabSOCS has serious restrictions regarding the number of possible major elements that can be specified for each sample, which can imply inaccuracies regarding the problem sample mass attenuation coefficient and, therefore, the problem sample *FEPE* obtention for problem samples characterized by containing a great number of major elements.
   - 4.2 In the case of EFFTRAN, the main advantage is the relatively wide range that can be addressed regarding detector types and being possible to use data from two software, Genie 2000 and Gamma Vision, to obtain problem sample *FEPE*. However, the need to transform the calibration sample *FEPE* to the problem sample *FEPE* as well as its respective experimental measurement which requires further sample pretreatment and analysis. In addition, it is needed to use a fit function for the problem sample *FEPEs*, and no option to include desired energies in the *FEPE* obtention which makes possible deviations in the *FEPE* values at those energies that are not considered in the fit.
   - 4.3 When using DETEFF, the main advantage is the simplicity of its usage being also possible to select relatively complex geometry

such as Marinelli. However, the number of possible detector types to be selected is relatively limited.

4.4 When using PENELOPE and Geant4, the main advantage versus the other simulation codes is the possibility to consider the entire physical process for the photon passage through material and its interaction with matter, making the problem sample *FEPE* simulation be more realistic. However, the design of code lines to run simulations using these two codes can be quite tedious and the computational cost can be relatively high.

4.5 The main advantage of using LabSOCS, DETEFF, PENELOPE and Geant4 versus EFFTRAN is the non-need to transform the calibration sample *FEPE* to the problem sample *FEPE*, which is directly obtained when using those other simulation codes. Another difference that can be extracted from that same comparison is the non-need to experimentally the calibration sample for the problem sample *FEPE* obtention. This can be considered as a disadvantage of EFFTRAN versus the other simulation codes, but it can also be considered as an advantage since the simulated problem sample *FEPEs* can be more realistically obtained when considering the real physical and chemical aspects regarding possible inhomogeneities of their compaction level and chemical composition.

4.6 In the case of using simulated methodologies, there is a clear advantage versus experimental methodologies which is the consideration of a very wide range of angles formed between photon trajectories and coaxial or radial detector axis in the case of coaxial or well-type detectors, respectively. This makes the self-attenuation effect corrections using simulated methodologies have a wider validity range versus experimental methodologies regarding possible problem sample chemical composition and apparent densities to be addressed.

5. Regarding comparisons among *FEPEs* obtained using simulated and experimental methodologies, different conclusions can be extracted.

5.1 Among Geant4, EFFTRAN and LabSOCS, statistically compatible results were obtained, however a clear underestimation of radionuclide concentration at low energies was observed using EFFTRAN, which is due to an overestimation of simulated *FEPE*.

5.2 Agreement between *FEPE*s obtained using DETEFF and experimental methods was obtained, as well as for PENELOPE case.

Declaration of competing interest

The authors declare that they have no known competing financial interests or personal relationships that could have appeared to influence the work reported in this paper.

Data availability

Data will be made available on request.

References

Alakangas, E., 2015. Quality guidelines of wood fuels in Finland VTT-M-04712-15. technical report. https://doi.org/10.13140/RG.2.1.3290.3127.

Appleby, P.G., Richardson, N., Nolan, P.J., 1992. Self-absorption corrections for well-type germanium detectors. Nucl. Instrum. Methods Phys. Res. Sect. B Beam Interact. Mater. Atoms 71 (2), 228–233.

Barba-Lobo, A., 2025. A new and general efficiency calibration methodology for Ge detectors using LabSOCS. Radiat. Meas. 181, 107374.

Barba-Lobo, A., Bolívar, J.P., 2022. A practical and general methodology for efficiency calibration of coaxial Ge detectors. Measurement 197, 111295. https://doi.org/10.1016/j.measurement.2022.111295.

Barba-Lobo, A., San Miguel, E.G., Lozano, R.L., Bolívar, J.P., 2021a. A general methodology to determine natural radionuclides by well-type HPGe detectors. Measurement 181 109561. https://doi.org/10.1016/j.measurement.2021.109561.

Barba-Lobo, A., Mosqueda, F., Bolívar, J.P., 2021b. An upgraded Lab-based method to determine natural γ-ray emitters in NORM samples by using Ge detectors. Measurement 186, 110153. https://doi.org/10.1016/j.measurement.2021.110153.

Barba-Lobo, A., Mosqueda, F., Bolívar, J.P., 2021c. A general function for determining mass attenuation coefficients to correct self-absorption effects in samples measured by gamma spectrometry. Radiat. Phys. Chem. 179, 109247. https://doi.org/10.1016/j.radphyschem.2020.109247.

Barba-Lobo, A., Gutiérrez-Álvarez, I., San Miguel, E.G., Bolívar, J.P., 2023a. A methodology to determine ^{212}Pb, ^{212}Bi, ^{214}Pb and ^{214}Bi in atmospheric aerosols; Application to precisely obtain aerosol residence times and Rn-daughters' equilibrium factors. J. Hazard Mater. 445, 130521. https://doi.org/10.1016/j.jhazmat.2022.130521.

Barba-Lobo, A., Expósito-Suárez, V.M., Suárez-Navarro, J.A., Bolívar, J.P., 2023b. Robustness of LabSOCS calculating Ge detector efficiency for the measurement of radionuclides. Radiat. Phys. Chem. 205, 110734. https://doi.org/10.1016/j.radphyschem.2022.110734.

Barba-Lobo, A., Expósito-Suárez, V.M., Suárez-Navarro, J.A., Bolívar, J.P., 2024. A new methodology for efficiency calibration of uncharacterized detectors by using characterized detectors. Radiat. Phys. Chem. 221 (7–8), 111763.

Budak, G., Karabulut, A., Sßimsßek, O., Ertugrul, M., 1999. Measurement of total atomic attenuation, total atomic photoelectric and total atomic scattering cross sections in the range 40≤ Z ≤52. NIMB 49, 379–382.

Canberra Industries, 2004. Genie 2000 Spectroscopy Software: Customization Tools, Printed in the United States of America.

Canberra Industries, 2012. Geometry composer User's manual. Canberra Industries. Meriden.

Civilbolg, 2015. https://civilblog.org/2015/01/06/how-to-reduce-gross-aggregate-sample-to-test-sample-by-quartering-or-coning-method/.

Cutshall, H., Larsen, I.L., Olsen, C.R., 1983. Direct analysis of ^{210}Pb in sediment samples: self-absorption corrections. Nucl. Instrum. Methods Phys. Res. Sect. A Accel. Spectrom. Detect. Assoc. Equip. 206, 309–312. https://doi.org/10.1016/0167-5087(83)91273-5.

De Francesco, A.M., Bocci, M., Crisci, G.M., 2018. Application of non-destructive XRF method to the study of the provenance for archaeological obsidians from Italian, Central European and South American sites. Quat. Int. 468, 101–108.

Díaz, N.C., Vargas, M.J., 2008. DETEFF: an improved Monte Carlo computer program for evaluating the efficiency in coaxial gamma-ray detectors. Nucl. Instrum. Methods Phys. Res. Sect. A Accel. Spectrom. Detect. Assoc. Equip. 586 (2), 204–210. https://doi.org/10.1016/j.nima.2007.11.072.

Diaz, N.C., Vargas, M.J., 2010. Improving the trade-off between simulation time and accuracy in efficiency calibrations with the code DETEFF. Appl. Radiat. Isot.: including data, instrumentation and methods for use in agriculture, industry and medicine 68 (7–8), 1413–1417. https://doi.org/10.1016/j.apradiso.2009.11.021.

DIFFRAC, 2016. https://www.bruker.com/en/products-and-solutions/diffractometers-and-x-ray-microscopes/x-ray-diffractometers/diffrac-suite-software/diffrac-eva.htmlDIFFRAC.EVA.

Gačnika, J., Sarapb, N.B., Mazeja, D., Prosenc, H., Štroka, M., 2019. Liquid scintillation counter calibration approach for 90Sr detection and testing performance of TK100 resin. Appl. Radiat. Isot. 151, 111–115.

Guerra J, G., Rubiano J, G., Winter, G.G., Guerra, A., Alonso, H., Arnedo, M.A., Tejera, A., Gi, l J.M., Rodríguez, R., Martel, P., Bolívar, J.P., 2015. A simple methodology for characterization of germanium coaxial detectors by using Monte Carlo simulation and evolutionary algorithms. J. Environ. Radioact. 149, 8–18. https://doi.org/10.1016/j.jenvrad.2015.06.017.

Guerra J, G., Rubiano J, G., Winter, G.G., Guerra, A., Alonso, H., Arnedo, M.A., Tejera, A., Mosqueda, F., Martel, P., Bolívar, J.P., 2018. Automatic Modeling Using PENELOPE of Two HPGe Detectors Used for Measurement of Environmental Samples by γ-spectrometry from a Few Sets of Experimental Efficiencies. Nuclear Instruments and Methods in Physics Research Section A: Accelerators, Spectrometers, Detectors and Gouda M M.

Hasan, M.M., Vidmar, T., Rutten, J., Verheyen, L., Camps, J., Huysmans, M., 2021. Optimization and validation of a LaBr3(Ce) detector model for use in Monte Carlo simulations. Appl. Radiat. Isot. 174, 109790.

Iuriana, A.R., Millwardb, G.E., Simac, O., Taylora, A., Blakea, W., 2018. Self-attenuation corrections for Pb-210 in gamma-ray spectrometry using well and coaxial HPGe detectors. App. Radiat. Isot. 134, 151–156.

Karasaka, A., 2021. Determination of major, minor, and toxic elements in tropical fruits by ICP-OES after different microwave acid digestion methods. Food Anal. Methods 14, 344–360.

Lei, Z., Pavia, S., Wang, X., 2024. Alkali-fusion as an effective method for activating low-reactivity silicate wastes: a comparative study. Constr. Build. Mater. 449, 138504.

Liao, X., Hu, Z., Luo, T., Zhang, W., Liu, Y. Zong, Zhou, K., Zhang, L., 2019. Determination of major and trace elements in geological samples by laser ablation solution sampling-inductively coupled plasma mass spectrometry. J. Anal. At. Spectrom. 34, 1126.

Modarresi, S., Masoudi, F., Farhadd, M., Karimi, 2018. A method for self-attenuation and sample-height correction for counting efficiency of HPGe using Marinelli beaker geometry. J. Radioanal. Nucl. Chem. 316, 129–137, 2018.

Moradi, F., Uddin, M., Alrefae, T., Ramazanian, H., Bradley, D.A., 2019. Monte Carlo simulations and analysis of transmitted gamma ray spectra through various tissue phantoms. Appl. Radiat. Isot. 146, 120–126. https://doi.org/10.1016/j.apradiso.2019.01.031.

OMNIAM, 2022. Ajuste e incertidummbres asociadas al método semicuantativo WDXRF OMNIAM.

Ramos-Lerate, I., Barrera, M., Ligero, R.A., Casas-Ruiz, M., 1999. A new method for gamma-efficiency calibration of voluminal samples in cylindrical geometry. J. Environ. Radiat. 38, 47–57.

Vidmar, T., Kanisch, G., Vidmar, G., 2011. Calculation of true coincidence summing corrections for extended sources with EFFTRAN. Appl. Radiat. Isot. 69 (6), 908–911. https://doi.org/10.1016/j.apradiso.2011.02.042.

Vraničar, J., Todorovi, N., Maksimović, I., Mladenovi, M., Mrđa, D., Travar, M., 2021. Testing of EFFTRAN and Angle software in comparison to GEANT 4 simulations in gamma spectrometry of cylindrical and noncylindrical sample geometries. NIMA 986, 164768.

Vraničar, A., Nikolov, J., Lazarević, Đ., Rikalo, A., Todorović, N., Arbutina, D., Travar, M., March 2022. Sample matrix influence on the efficiency function modeling for uranium isotopes determination by gamma spectrometry. Radiat. Phys. Chem. 192, 109891.